

Detector for LWIR Hyperspectral Imagers.

D. J. Lees^{*}, D. Barron[†], J. W. Cairns^{*}, P. C. Haynes^{*} and C. J. Hollier^{*}

^{*}QinetiQ Ltd, St Andrews Road, Malvern, Worcs. WR14 3PS

[†]Thales Optronics, Thorpe Road, Staines, Middlesex. TW18 3HP

Abstract

This project is aimed at supporting UK industry to produce a low Noise Equivalent Temperature Difference (NETD) hyperspectral long waveband IR camera for the UK MoD that does not require cryogenically cooled optics, is compact and relatively low in cost. During the first year this project has concentrated on modelling the performance of the hyperspectral camera, and the design of a linearly variable filter (LVF) and readout integrated circuit (ROIC). Modelling has shown that an NETD of 78mK for a 48 band system and 43mK for a 24 band system should be achievable. The LVF specification has been agreed and a contract is in place for manufacturing samples. Two types of ROIC pixel have been designed; a direct injection circuit and a chopper stabilised amplifier. The array addressing architecture is the same in both cases. Stray radiation modelling has shown that a revised cold shield design should reduce the background pedestal by a factor of 5 when compared with the earlier Hyperion camera.

Keywords: hyperspectral, long waveband infrared,

Introduction

Hyperspectral sensing has the potential to improve false target rejection by an order of magnitude over conventional broadband systems. A significant amount of investment has been made in the processing of infrared (IR) hyperspectral data with good results. However, the data that has been collected has derived from research instruments that have cryogenically cooled optics. These are bulky and expensive. This project is aimed at supporting UK industry to produce a low Noise Equivalent Temperature Difference (NETD) hyperspectral long waveband IR camera for the UK MoD that does not require cryogenically cooled optics, is compact and relatively low in cost.

Hyperspectral camera system

Figure 1 shows the key components of the hyperspectral camera system. The optical

system, which was designed and built under the UK MoD Hyperion project, contains a novel optical component known as a grism. The grism diffracts the spectral content of each point in the scene and spreads it out along one dimension of the focal plane. Two grisms will be available with diffraction wavelength shifts of 1nm and 2nm per 1 μ m on the focal plane. Both grisms cover a wavelength band of 8.0 μ m to 10.4 μ m. For a 50 μ m pixel pitch focal plane array (FPA) this results in a camera with either 48 50nm wide bands or 24 100nm wide bands.

The second dimension on the FPA contains spatial information from one line in the scene. Multiple lines are acquired using a scanning mirror to build up a two dimensional image. Stray radiation is minimised by the use of a linearly variable filter (LVF) and baffled cold shield as described in the following sections. A Stirling cycle engine is used to cool the

custom built long waveband IR (LWIR) FPA.

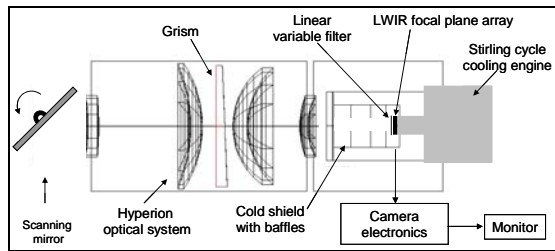


Figure 1 Hyperspectral camera system

The thermal performance of the hyperspectral camera has been modelled with an optimised cold shield and a linearly variable filter (LVF). Results show that thermal sensitivities of 78mK (48 band system) and 43mK (24 band system) can be achieved. The hyperspectral cube update rate for both systems is approximately 2.5Hz.

Linear Variable Filter

The LVF is designed to transmit radiation from the target and attenuate flux from other sources such as the optical system, dewar component, and Stirling engine. By reducing flux from these sources the focal plane array stare time can be increased resulting in lower NETD.

The diffraction pattern at the focal plane from the 1nm per 1 μ m grism is shown schematically in figure 2. In the horizontal (spatial) direction the centre frequency is required to remain constant along the spatial axis.

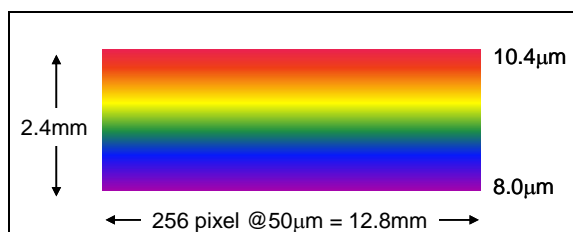


Figure 2 Radiation pattern from the grism

The LVF needs to be designed to transmit the radiation pattern from the grism (and therefore the target) and attenuate all other wavelengths.

To reduce spectral crosstalk the distance between the LVF and detector array needs to be minimised. This can be achieved either by mechanically mounting a separate LVF as close to the detector array as possible or by the deposition of the LVF layers directly onto the detector array substrate. This project will initially concentrate on the separate LVF approach whilst in parallel conduct a feasibility study on direct deposition options.

Infrared long waveband focal plane arrays

IR long waveband FPAs for the hyperspectral camera will be fabricated at QinetiQ Malvern. Each FPA consists of two main components, an array of IR detectors and a custom silicon readout integrated circuit (ROIC). FPAs are fabricated by bump bond hybridising detector array to ROICs.

IR detector arrays will be fabricated in year two of this project (FY08). These arrays will be based on cadmium mercury telluride (CMT) grown on silicon substrates, a technology pioneered by QinetiQ. Arrays will be fabricated using dry and wet etching technology to form mesa devices.

Two ROIC variants have been designed over the last year; these are described in the following paragraphs.

The direct injection pixel circuit, shown in figure 3, is commonly used in high performance broad band IR FPAs.

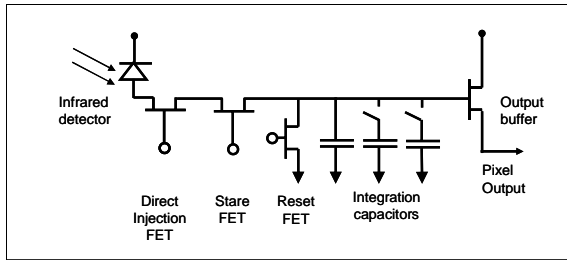


Figure 3 Direct injection pixel circuit

The LWIR detector is biased at close to 0 volts by the common gate direct injection MOSFET. The stare MOSFET controls the time over which the integration capacitors store the current generated by the detector. At the end of the stare time the voltage on the integration capacitors is read out via the output buffer. Finally the voltage on the integration capacitors is discharged using the reset MOSFET.

Three integration capacitors have been used in this design to increase the dynamic range. For example, all three can be used under high signal condition and only one used when there is a low signal level.

Due to the low photon flux from the narrow band hyperspectral system, there is a risk that this circuit will have poor injection efficiency. This risk is reduced by cooling the FPA to 65K using a Stirling cycle engine or by using a chopper stabilised amplifier in the pixel circuit.

The chopper stabilised amplifier is designed to improve the charge injection efficiency from the photo-detector into the pixel circuit. The circuit works by wrapping a voltage gain unit around the common gate direct injection MOSFET in a configuration known as feed-forward as shown schematically in figure 4.

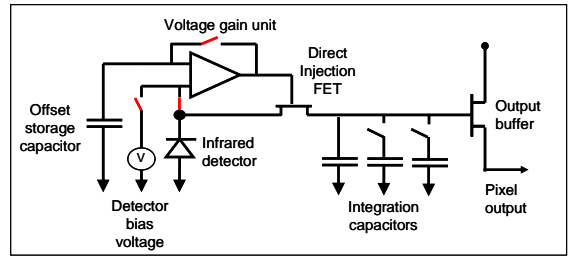


Figure 4 Chopper stabilised amplifier

The input impedance of the pixel circuit is reduced by a factor equal to the voltage gain, which is typically x100.

The MOSFETs used in the voltage gain unit have significant low frequency (or 1/f) noise which, if not removed, will degrade the focal plane array performance. The chopper stabilised amplifier rejects the low frequency components by sampling the input noise at the start of each frame readout and storing the value on an in-pixel capacitor. The noise level is then subtracted from the photo-signal during the stare time.

Whilst the chopper stabilised amplifier offers the highest performance, ROICs with direct injection circuits will also be fabricated for risk reduction.

The pixel array addressing architecture for both types of pixels is shown in figure 5.

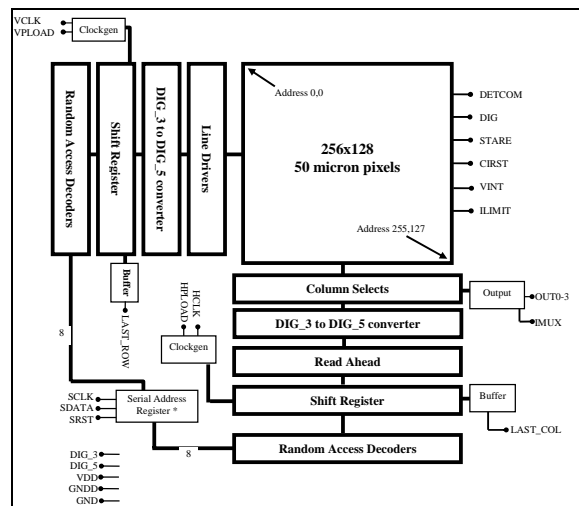


Figure 5 ROIC architecture

Pixels can be addressed by raster scanning the whole array or by random accessing sub-array windows. There are four analogue output channels each capable of supporting 10M pixels/s data rates.

A Cadence design system at QinetiQ Malvern has been used to design and layout the ROICs. The ROICs will be fabricated at a silicon foundry using a 0.6 μ m minimum feature size process and delivered to QinetiQ for assessment.

Stray radiation modelling

The radiometric model is constructed using a series of geometric shapes enclosing the optical elements. These shapes radiate energy at 15 discrete wavelengths with the spectral intensity being determined by their temperature. Whilst the principal ray path from the slit to the FPA is determined by the combination of refraction and first order diffraction at the grism, there are numerous other paths created by reflection at lens surfaces and higher order diffraction in the grism.

The optical system components are similarly radiating energy which can also reach the focal plane by these mechanisms. The aim is to design a FPA cold shield that minimises the number of paths by which this radiation can reach the focal plane. This stray radiation needs to be absorbed in the cold shield to prevent it from reaching the FPA. Consequently, an efficient design of the baffling, both inside and outside the cold shield, is vital for minimising stray radiation. Figure 6 shows an example of the baffles being used in the model.

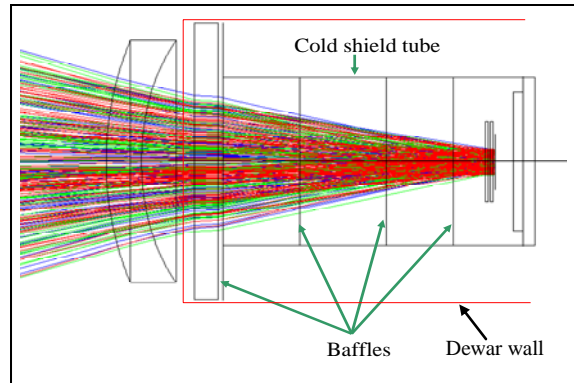


Figure 6 Ray tracing of cold shield with baffles

These baffles are arranged as three annuli at appropriate positions within the cold shield. A larger baffle, which extends from the cold shield aperture to the dewar wall, has been included to prevent radiation from the dewar cavity intercepting the FPA. Radiation from the inside of the spectrometer and from the ambient environment will be absorbed by these cold sections.

A further aim of this activity was to improve the modelling of the radiation from both the germanium and gallium arsenide lens elements, and the germanium grism. This improvement was necessary to determine whether the radiation from these components significantly contributes to the pedestal level.

Results from this recent work have confirmed that the major source of pedestal in the Mk.2 version of the Hyperion camera is the retro reflection of ambient radiation. This radiation enters the spectrograph via the gap between the window and the external cold mirror. Closing this gap and using a more efficient cold shield reduces the pedestal contribution from the ambient radiation by a factor of approximately 5. Figure 7 shows the modelled ray tracing of both the original Hyperion demonstrator and the improved cold shield design.

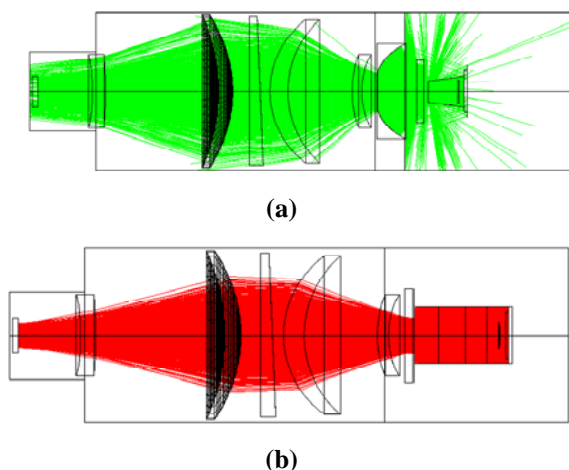


Figure 7 Ray tracing of optical system with (a) original Hyperion demonstrator cold shield with baffles and (b) optimised cold shield design

Table 1 shows a breakdown of the stray radiation contributions from key regions in the optical system.

This suggests that an overall pedestal reduction of x10 is feasible, but a factor of x5 seems more likely when an allowance for non-modelled imperfections is included.

Radiation source	Radiation flux incident on detector (W)	
	Original Hyperion Optical System	Improved design
Outer Barrel	2.4E-02	2.0E-03
Left hand outer barrel	5.0E-07	4.0E-06
Centre 1 outer barrel	8.0E-04	2.7E-04
Centre 2 outer barrel	8.6E-03	1.8E-05
Right hand outer barrel	0.0E+00	0.0E+00
Mirror cavity cylinder	7.0E-04	1.0E-03
Mirror cavity end	5.4E-05	4.1E-06
Total	3.5E-02	3.3E-03

Table 1 Radiation flux incident on detector

Conclusions

During the first year this project has concentrated on modelling the performance of the hyperspectral camera and the design of an LVF and ROIC.

Modelling has shown that an NETD of 78mK for the 48 band system and 43mK for the 24 band system should be achievable. The hyperspectral cube update rate for both of these configurations is approximately 2.5Hz.

The LVF specification has been agreed and a contract is in place for manufacturing samples.

Two types of ROIC pixel have been designed; a direct injection circuit and a chopper stabilised amplifier. The array addressing architecture is the same in both cases. These ROICs will be hybridised to CMT detector arrays during FY08.

Stray radiation modelling has shown that a revised cold shield design should reduce the background pedestal by a factor of 5 when compared with the earlier Hyperion camera.

Acknowledgements

The work reported in this paper was funded by the Electro-Magnetic Remote Sensing (EMRS) Defence Technology Centre, established by the UK Ministry of Defence and run by a consortium SELEX Sensors and Airborne Systems, Thales Defence, Roke Manor Research and Filtronic.